A Mesoporous Silica-Based Nano-Drug Co-Delivery System with Gemcitabine for Targeted Therapy of Pancreatic Cancer

Quan Lin, Shiwei Guan, Minghui Peng and Haibo Yu

Department of Hepatobiliary Surgery, Wenzhou Central Hospital, The Dingli Clinical Institute of Wenzhou Medical University, Wenzhou, Zhejiang, China

ABSTRACT

Objective: To investigate the efficacy and safety of the mesoporous silica-based nano-drug co-delivery system with gemcitabine (GEM) in the treatment of pancreatic cancer.

Study Design: Experimental study.

Place and Duration of the Study: Wenzhou Central Hospital, Zhejiang Province, China, between July 2022 and November 2023.

Methodology: Ce6@MSN-Fe_3O_4/GEM@DPM nanoparticles were prepared and structurally characterised, then their drug loading and entrapment efficiency were calculated, and *in vitro* drug release and cytotoxicity assays were performed. In addition to that, mesoporous silica nanorods were prepared and structurally characterised for cellular uptake, cytotoxicity, and reactive oxygen species detection.

Results: The mesoporous silica nanoparticles were spherical in shape and possessed a unique core-shell structure. The prepared nanoparticles had good entrapment efficiency and drug loading, and exibited pharmacotoxic and phototoxic effects on cells. The mesoporous silica nanorods were taken up by pancreatic cancer cells and exbitied cytotoxicity.

Conclusion: Mesoporous silica-based nano-drug co-delivery system, which carries GEM, is an effective targeted drug delivery system to provide new research ideas for the treatment of pancreatic cancer.

Key Words: *Pancreatic cancer, Gemcitabine, Magnetic nanocomposites, Photodynamic therapy, Targeted drug delivery.*

How to cite this article: Lin Q, Guan S, Peng M, Yu H. A Mesoporous Silica-Based Nano-Drug Co-Delivery System with Gemcitabine for Targeted Therapy of Pancreatic Cancer. *J Coll Physicians Surg Pak* 2024; **34(12)**:1456-1463.

INTRODUCTION

Pancreatic cancer (PC) is presently considered to be one of the most highly malignant tumours worldwide, with a 5-year survival rate of less than 10% after diagnosis.[1] PC has now become the fourth most common cause of death among cancer patients in the United States.[2] PC can only be treated surgically. Unfortunately, early symptoms are scarce, leading to most patients being diagnosed in the middle-to-late stages of the disease. Only a small fraction of patients, around 10-15%, can undergo a radical resection.[3] Chemotherapy is a crucial method of clinical treatment for PC. However, the chemotherapeutic drugs commonly used in clinical practice not only eliminate tumour cells but also inflict extensive damage on normal tissues and cells, resulting in severe systemic toxicity and reducing clinical efficacy.[4]

Correspondence to: Dr. Haibo Yu, Department of Hepatobiliary Surgery, Wenzhou Central Hospital, The Dingli Clinical Institute of Wenzhou Medical University, Wenzhou, Zhejiang, China
E-mail: zjuboby@zuaa.zju.edu.cn

Received: February 12, 2024; Revised: October 06, 2024; Accepted: November 01, 2024
DOI: https://doi.org/10.29271/jcpsp.2024.12.1456

Therefore, exploring ways to decrease the harm caused by chemotherapeutic drugs to normal tissue sites is a valuable pursuit. Additionally, chemotherapy resistance remains a significant factor contributing to the bleak prognosis of PC.

Gemcitabine (GEM) remains the go-to chemotherapy for PC and is commonly used as a first-line treatment. It has proven effective in patients with advanced and metastatic PC.[5] However, PC cells show greater resistance to GEM compared to other chemotherapy types, which severely limits the effectiveness of GEM. GEM, a cytidine analogue, enters the body and produces difluorocytidine diphosphate and difluorocytidine triphosphate. These metabolites have various inhibitory effects on DNA synthesis. Resistance to GEM is influenced by various factors, including the acquired and/or intrinsic pathways, dense heteroproliferative stroma that acts as a barrier to vascular perfusion and drug permeability, changes in drug metabolism kinetics, interactions between tumour cells and the tumour microenvironment, and metabolic impacts of microorganisms within the tumour.[6-9] In order to improve the efficacy of GEM, two routes have been identified: One is to improve the biostability and bioavailability of GEM by chemical modification of GEM; the other is to prepare GEM-loaded nanomedicines in order to improve the efficiency of drug delivery.[10]

In recent years, nanotechnology and nanomaterials have received extensive attention from scholars. Nanocarrier-based drug delivery methods have enhanced bioavailability, reduced side effects, and provided a viable solution for the improved treatment of PC.[11] Several drug delivery nanocarriers have been described; however, mesoporous silica nanoparticles (MSN) are now frequently used due to their porous structure which provides a high cargo-loading capacity. Therefore, the authors attempted to construct a magnetic mesoporous silica nanoparticle with a unique core-shell structure that can carry GEM to enhance the loading and releasing ability of the drug, improve the anti-tumour effect and reduce the systemic toxicity and side effects of GEM in pancreatic cancer patients, and provide further guidance for the clinical treatment of pancreatic cancer. The objective of this study was to investigate the efficacy and safety of the mesoporous silica-based nano-drug co-delivery system with GEM in the treatment of pancreatic cancer.

METHODOLOGY

This is an experimental study conducted between July 2022 and November 2023 at Wenzhou Central Hospital, China. Chemicals including 3-aminopropyltriethoxysilane (APTES), cetyltrimethylammonium bromide (CTAB), ammonia (28%), ammonium ferrous sulphate (99.5%), sodium hydroxide (NaOH), oleic acid (OA), 2-bromo isobutyric acid (BMPA), citric acid, N,N'-dicyclohexylcarbodiimide (DCC), dihydroporphine E6 (Ce6), n-hexane, tetraethyl silicate (TEOS), hydrochloric acid (37%), gemcitabine hydrochloride, methanol, ammonium acetate, glacial acetic acid, acetonitrile, and trifluoroacetic acid anhydrous ethanol was obtained from Macklin (Shanghai, CHN). The 1640 medium, foetal bovine serum (FBS), trypsin, phosphate buffer, penicillin-streptomycin, phosphate-buffered saline (PBS), Cell Counting Kit-8, Reactive Oxygen Detection Kit CHN, Fluorescein Isothiocyanate (FITC), and PANC02 cells were obtained from various vendors.

CTAB was dissolved in ultrapure water, and dispersed in anhydrous ethanol after dropwise addition of concentrated ammonia. APTES was added dropwise, and then Fe_3O_4-Br alcohol dispersion system was added. MSN-Fe_3O_4 nanoparticles were obtained after drying. MSN-Fe_3O_4 was taken up and dispersed in dimethyl formamide (DMF) solution, followed by the addition of DCC and Ce6. Ce6@MSN-Fe_3O_4 composite nanoparticles were obtained after separation and collection. Finally, MSN-Fe_3O_4 and dimethyl propanol (DPM) were mixed and added to the GEM solution. Ce6@MSN-Fe_3O_4/GEM@DPM nanoparticles were obtained after lyophilisation and characterised using transmission electron microscopy (Figure 1).

A Ce6 control sample was weighed and diluted in a series of standard solutions. The standards and the supernatant washed with DMF were collected and injected into the high performance liquid chromatography (HPLC) system for analysis. The free Ce6 content was measured, and the loading was calculated.

GEM control sample was weighed and diluted in a series of standard solutions. The prepared Ce6@MSN-Fe_3O_4/GEM@DPM nanosolutions loaded with GEM were placed in a dialysis bag to obtain the dialysis medium. The standard solution and dialysis medium were collected, filtered, and injected into an HPLC system to calculate the entrapment efficiency and drug loading.

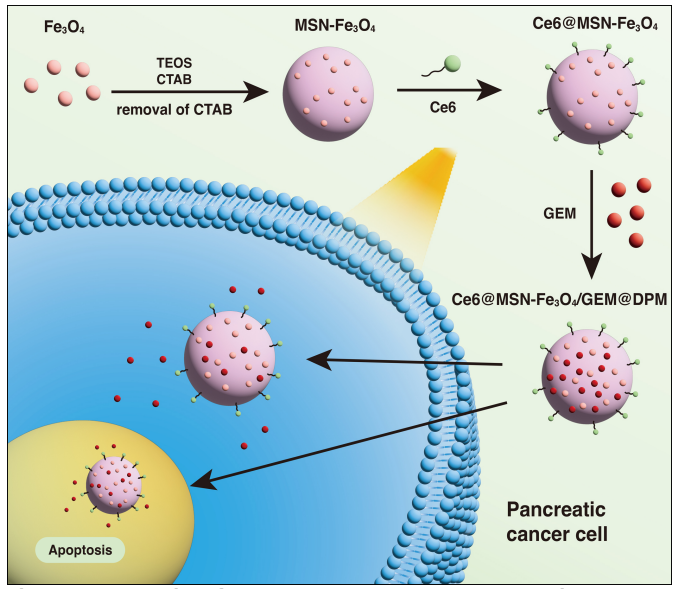

Figure 1: Preparation of Ce6@MSN-Fe_3O_4/GEM@DPM composite nanoparticles and *in vitro* anti-tumour process schema.

The appropriate amount of GEM control was weighed and diluted into a series of standard solutions. Ce6@MSN-Fe_3O_4/GEM@DPM dry powder was weighed and dissolved in PBS buffer of pH 7.4 and 6.0 and solutions were prepared at fixed time intervals. The standard and buffer solutions were collected, filtered, and injected into an HPLC system to plot the *in vitro* drug release profile.

To observe the uptake of Ce6@MSN-Fe_3O_4/GEM@DPM by PANC02 cells, PANC02 cells in the logarithmic growth phase were taken and cultured in the first method. Once the cells grew to 85%, the culture medium was replaced with Ce6@MSN-Fe_3O_4/GEM@DPM culture medium. Primary staining was performed using hydrogen peroxide acetate and embedded blocks were prepared after ethanol dehydration. The embedded blocks were sectioned into slices and placed on a carbon support membrane. After staining with lead citrate and restaining with dioxyl acetate, the samples were analysed by transmission electron microscopy. In the second method, PANC02 cells in logarithmic growth phase were harvested and cultured with free Ce6, Ce6@MSN-Fe_3O_4, and Ce6@MSN-Fe_3O_4/GEM@DPM culture medium. After fixation, washing, and incubation, the 6-well plates were photographed using an upright fluorescence microscope.

To detect the role of nanocomplexes in apoptosis, PANC02 cells were taken from the logarithmic growth phase and treated with Ce6 and Ce6@MSN-Fe_3O_4. A blank control group was set up, with cells only without any stimulus and a solvent control group included only culture medium. One of the plates was exposed to laser irradiation. After resuspension and incubation, the samples were analysed by flow cytometry.

To examine the cytotoxicity of nanocomplexes, cell suspensions were prepared from the passaged cells and inoculated. Ce6, Ce6@MSN-Fe_3O_4, GEM, and Ce6@MSN-Fe_3O_4, GEM@DPM containing GEM were given and the absorbance at 450 nm was detected with an enzyme marker after incubation.

The CTAB was dissolved in ultrapure water with stirring and concentrated ammonia was added dropwise. TEOS was then added dropwise into the reaction system to disperse the collected solid sample, which was subsequently dried to obtain mesoporous silica nanorods (MSNR). Characterisation was carried out using the transmission electron microscopy and a diffractometer.

To observe the uptake of MSNR by PANC02 cells, FITC was added to APTES and stirred, and dried MSNR was dispersed. MSNR-FITC was obtained by centrifugation. PANC02 cells in logarithmic growth phase and were collected, and a single cell suspension was prepared. The previous medium was replaced by MSNR-FITC culture medium, and the identical cell culture and treatment procedures were administered as for Ce6@MSN-Fe_3O_4/GEM@DPM in the previous part. The 6-well plate was photographed using an upright fluorescence microscope.

To examine the cytotoxicity of MSNRs, the passaged cells were harvested and prepared as a cell suspension, which was then treated with varying concentrations of the MSNR nanorod solution. At the end of the incubation period, the absorbance at 450 nm was determined using an enzyme marker.

For reactive oxygen species assay experiments, PANC02 cells in the logarithmic growth phase were incubated with different concentrations of the MSNR nanorod solution. Cells were incubated in DCFH-DA diluted with a serum-free culture medium. Detection was performed using flow cytometry.

Statistical analyses were conducted using SPSS version 22.0. Normally distributed measures were expressed as $\bar{x} \pm s$, and means between the two groups were compared using t-tests. Linear regression was used for regression analyses. GraphPad Prism 9.0 software was used for picture drawing. A value of $p < 0.05$ was considered statistically different.

RESULTS

Transmission electron microscopy (TME) results are shown in Figure 2(A-D). The synthesised MSN exhibits a regular spherical morphology with good dispersion, having an average dimension of approximately 260 nanometers. The sample exhibits a unique core-shell structure. The synthesised Fe_3O_4 nanocrystals assume a uniform spherical configuration with a particle diameter of around 50 nanometers. Through nucleophilic substitution reactions, it is apparent that Fe_3O_4 nanoparticles are modified onto the MSN, resulting in Ce6@MSN-Fe_3O_4 nanoparticles. After DPM modification, Ce6@MSN-Fe_3O_4/GEM@DPM nanoparticles are obtained. As depicted, liposome copolymers encapsulate the outermost layer of the sample, presenting a well-defined spherical shape, excellent dispersion, no agglomeration, and uniform particle size distribution, indicating the successful preparation of Ce6@MSN-Fe_3O_4/GEM@DPM composite nanoparticles. Then, a regression equation was established: $y = 20.611x + 57.673$, 1~100 μg/mL, $R2 = 0.996$. Combining the corresponding standard curve, the calculated loading amount of Ce6 was 7.5%.

This study first established a regression equation: $y = 17.435x + 60.696$, 1~100 μg/mL, $R2 = 0.997$. Combining the corresponding standard curve, the calculated ER of GEM was 83.9%, and the DL was 21.0% (Figure 2(E-G)). Subsequently, *in vitro* drug release experiments were conducted. The *in vitro* release profile depicts the cumulative release of GEM from Ce6@MSN-Fe_3O_4/GEM@DPM under varying pH conditions. The experimental results showed that the release rate of Ce6@MSN-Fe_3O_4/GEM@DPM increased in acidic medium at pH 6.0, indicating that lipids undergo swelling in acidic medium, promoting more drugs to be released from the pore channel. Due to the buffering effect of lipid silica nanoparticles, GEM was released relatively slowly in pH 7.4 medium.

The TEM image revealed that the nanoparticles were internalised into the cells, indicating that the synthesised composite nanoparticles could be effectively taken up by PANC02 cells (Figure 2(H,I)). The fluorescence cell uptake experiment results demonstrate that the red fluorescence of Ce6-loaded MSN-Fe_3O_4 nanocomposites is significantly stronger than that of free Ce6, affirming that the Ce6-loaded nanocomposites can be effectively taken up by PANC02 cells. By comparing the uptake of free Ce6 and Ce6@MSN-Fe_3O_4 nanocomposites, it is observed that the red fluorescence of Ce6@MSN-Fe_3O_4/GEM@DPM is stronger and partially overlaps with the blue-stained nuclei, suggesting that Ce6@MSN-Fe_3O_4/GEM@DPM can efficiently enter the cytoplasm and cell nuclei, achieving drug enrichment and effective release.

In the absence of light exposure, both Ce6 and Ce6@MSN-Fe_3O_4 nanocomposites scarcely induce cell apoptosis (apoptotic percentage below 15%), and neither exhibits cellular toxicity. However, GEM and Ce6@MSN-Fe_3O_4/GEM@DPM both manifest significant cytotoxicity. Following light exposure, both Ce6 and Ce6@MSN-Fe_3O_4 nanocomposites induce cell apoptosis and demonstrate phototoxic effects. Compared to Ce6, Ce6@MSN-Fe_3O_4 nanocomposites induce cell apoptosis more significantly, which can better exert the phototoxicity of photosensitisers. Ce6@MSN - Fe_3O_4 / GEM@DPM nanocomposites have both drug toxicity and phototoxicity effects, thus exhibiting a more pronounced cell-killing effect (Figure 2 (J-M)).

TEM results are shown in Figure 3. Five MSNRs were randomly selected, and the average length and diameter of these rods were measured and recorded. The aspect ratio was calculated to be approximately 5.1. XRD is a technique that uses x-rays to obtain diffraction patterns from crystalline materials.

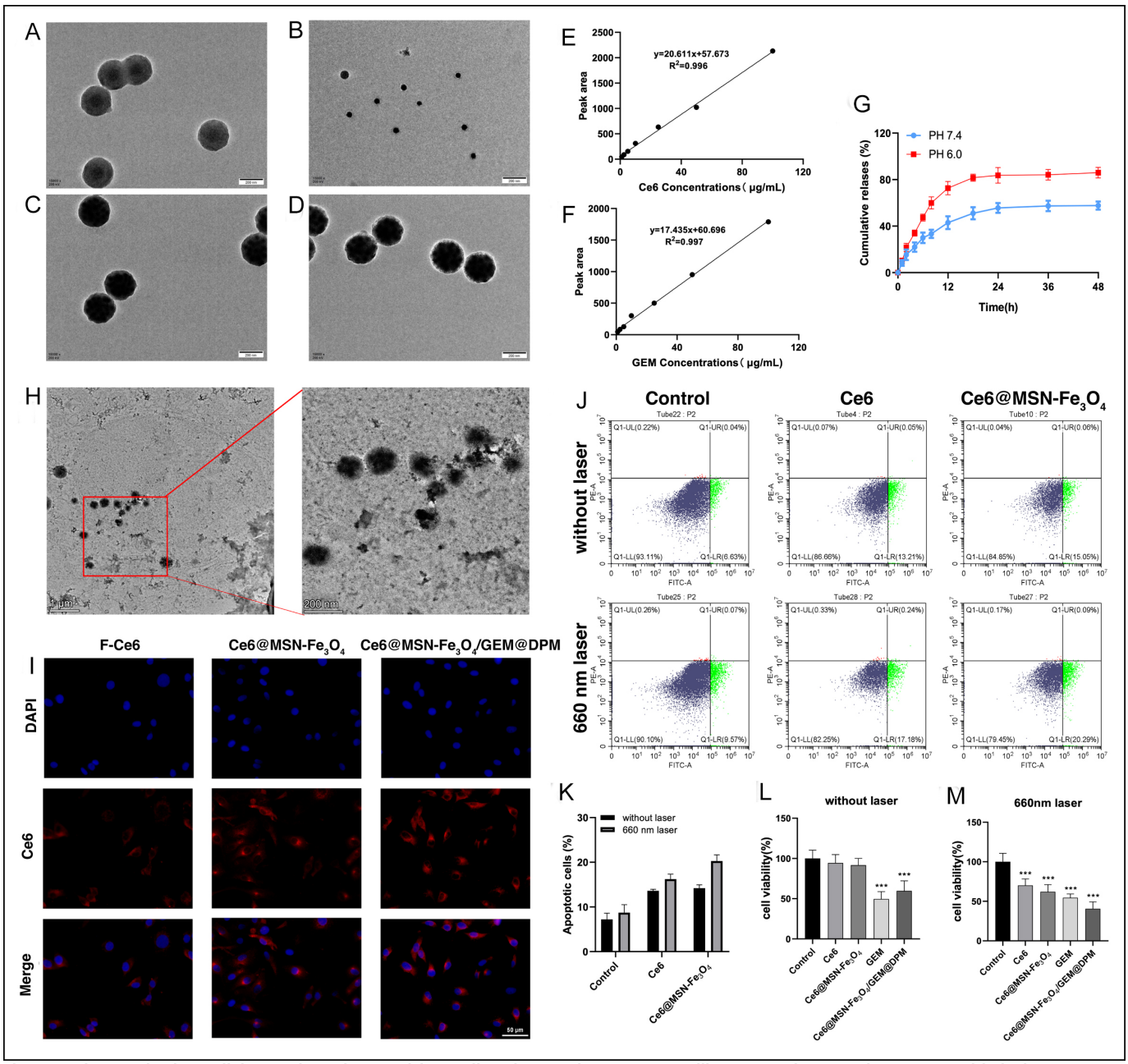

Figure 2: Characterisation, cellular uptake and cytotoxicity studies of magnetic mesoporous silica nanoco-drug-carrying systems with dual-porous core-shell structure (A-D). TEM results of MSN, Fe_3O_4 nanocrystals, Ce6@MSN-Fe_3O_4 and Ce6@MSN-Fe_3O_4/GEM@DPM. (E) Standard working curve for the determination of Ce6 standard solution in HPLC system. (F) Standard working curve for the determination of gemcitabine (GEM) standard solution in HPLC system. (G) *In vitro* drug release profile of Ce6@MSN-Fe_3O_4/GEM@DPM at different pH. (H) Results of TEM cell uptake. (I) Results of fluorescent cell uptake. (J,K) Ability of Ce6 and Ce6@MSN-Fe_3O_4 to induce apoptosis in the presence or absence of light. (L,M) Cytotoxicity of Ce6, Ce6@MSN-Fe_3O_4, GEM, and Ce6@MSN-Fe_3O_4/GEM@DPM in the presence or absence of light.

The diffraction pattern was obtained by processing the x-ray signal characteristics produced by the different degrees of diffraction phenomena that occur when the crystal is irradiated with x-rays. As shown in Figure 3B, the prepared MANR has three distinct diffraction peaks, corresponding to the (10), (11), and (20) planes of a p6mm two-dimensional hexagonal structure. The sharpness of the diffraction peaks indicates the formation of an ordered mesoscopic structure.

TEM was used for observing the uptake of MSNR by PANC02 cells. It was observed that MSNR were taken up by PANC02 cells. The uptake of MSNR silica rods by cells was also observed using the fluorescence microscopy. FITC was used to label and locate the MSNR. The results demonstrated that MSNR can traverse the cellular membrane of PANC02 cells, entring into the cell and distributing throughout the entire cytoplasm. Subsequently, CCK8 testing showed no significant cytotoxicity when the concentration of MSNR reached 100 μg/mL.

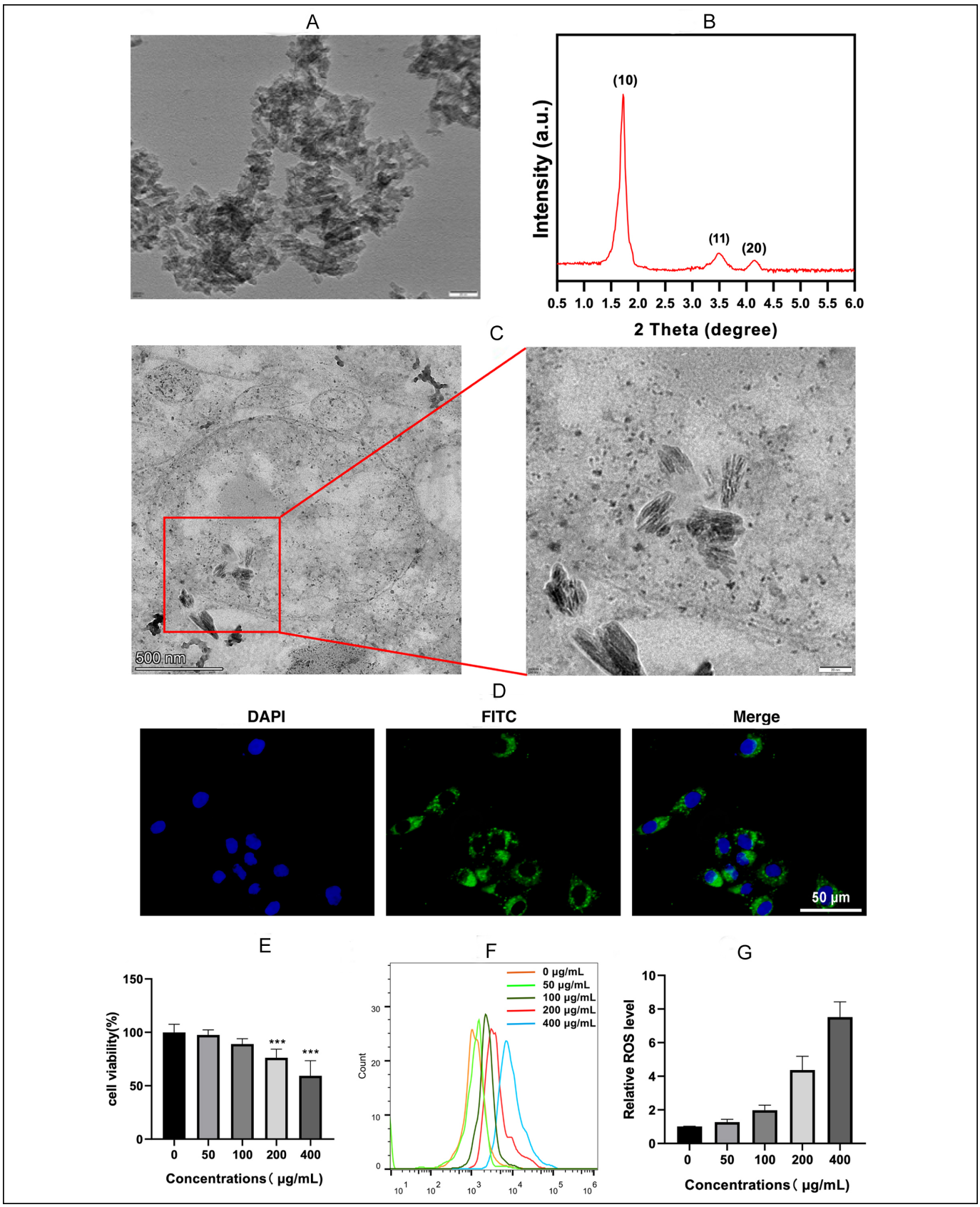

Figure 3: Characterisation, cellular uptake, and cytotoxicity studies of mesoporous silica nanorods (MSNR). (A) Results of TEM (B) Results of XRD. (C) Results of TEM cellular uptake. (D) Results of fluorescence cellular uptake. (E) Cellular survival at different concentrations of MSNR. (F, G) Oxidative stress levels of cells at different concentrations of MSNR.

However, as the concentration increased to 200 µg/mL, cytotoxic effects became evident. When the concentration further rose to 400 µg/mL, MSNR exhibited pronounced cytotoxicity, with cell viability at 59.3%. Furthermore, co-culturing MSNR with PANC02 cells resulted in a marked increase in intracellular ROS levels, showing a concentration-dependent relationship. This suggests that as the concentration of MSNR increases, it substantially elevates the cellular oxidative stress level.

DISCUSSION

Multidrug resistance (MDR) is a major obstacle to effective chemotherapy for many human malignancies. Nanoparticulate drug delivery systems have been reported to bypass MDR, but their therapeutic efficacy remains limited.[12] Over the past few decades, several targeted delivery strategies have been explored in pancreatic ductal adenocarcinoma, including liposomes, polylactic-co-glycolic acid-based polymer nanoparticles, solid lipid nanoparticles, and MSNs.[13] Among these, MSNs hold tremendous potential for drug delivery. MSNs have a customised mesoporous structure and a high specific surface area, which has significant advantages over traditional drug nano-carriers.[14] The core-shell ordered mesoporous silica nanoparticles have a cubic-structured core with ordered mesoporous channels, while the shell has divergent mesoporous channels, which have a high specific surface area and large pore volume. Moreover, the surface of the through-hole is rich in silicon hydroxyl groups, which may have a stronger drug loading capacity to meet the needs of multi-drug loading, and has the potential to become an excellent drug carrier.[15,16] The superparamagnetic behaviour of nanomaterials serves as a multitude of purposes in cancer diagnosis and treatment. Superparamagnetic Fe_3O_4 nanoparticles offer advantages such as excellent biocompatibility, biodegradability, and high magnetic saturation intensity, making them widely applicable in the biomedical field. Their applications encompass targeted drug delivery systems, magnetic photothermal therapy, and magnetic resonance imaging contrast agents.[17,18] In a research work, core-shell magnetic mesoporous silica nanoparticles (Fe_3O_4@MSN) were considered as potential therapeutic candidates.[18] PDT, on the other hand, is an optically-driven treatment method with a broad and non-specific cytotoxic mechanism, enabling it to provide significant killing of chemotherapy multidrug-resistant tumour cells.[19]

Therefore, in this study, Ce6@MSN-Fe_3O_4 composite nanoparticles were designed for carrying the GEM. The loading capacity of the photosensitiser Ce6 was determined, yielding a loading capacity of 7.5%. Subsequently, the authors prepared the composite nanoparticles containing GEM, and the structure of the composite nanoparticles was characterised by TEM, and the results showed successfully prepared Ce6@MSN-Fe_3O_4/GEM@DPM composite nanoparticles. To investigate the drug-loading performance of the composite nanoparticles on GEM, ER and DL of GEM were calculated, and the results showed that ER of GEM was 83.9% and the DL was 21.0%. This indicates that the designed Ce6@MSN-Fe_3O_4/GEM@DPM composite nanoparticles exhibit excellent entrapment efficiency and drug loading.

Tumour cells generate a substantial amount of lactate, resulting in acidification of the tumour microenvironment (TME), causing the pH within the TME to be lower than that of normal cells. This acidic TME can serve as an effective target for cancer therapy. The pH-responsive characteristics of the carrier will drive the selective accumulation of nanoparticles within tumour cells and trigger drug release, making it particularly suitable for targeted cancer drug delivery.[20] The *in vitro* drug release experiments reveal that Ce6@MSN-Fe_3O_4/GEM@DPM exhibits an increased drug release rate under acidic conditions with a pH of 6.0, while the release in a pH 7.4 medium is relatively slow. This indicates that more GEM is released from the nanoparticle pores in acidic TME, adapting to the acidic TME, and achieving its therapeutic effect on treating tumours.

Compared to conventional oncology therapies, photodynamic therapy (PDT) allows for relatively precise and efficient treatment with fewer side effects. In PDT, photosensitisers accumulate at cancerous sites. When these tissues are exposed to light of specific wavelengths, they generate singlet oxygen and other cytotoxic reactive oxygen species, leading to cellular apoptosis and/or necrosis.[11] Due to PDT's broad and nonspecific cytotoxic mechanism, it exerts a significant impact on chemotherapy-resistant tumour cells. Zhang *et al.* harnessed MSNs to co-load the chemotherapeutic drug cisplatin and the photosensitiser Ce6. This strategy facilitated the uptake of cisplatin by cisplatin-resistant lung cancer cells and effectively reversed the cisplatin resistance.[21] Ozge *et al.* found that Zn phthalocyanine-loaded mesoporous silica nanoparticles exhibit a high potential for the destruction of pancreatic cancer cells.[22] However, studies on magnetic mesoporous silica nanoparticles loaded with drugs and photosensitisers have not been reported more frequently. Some studies suggest excessive doses of photosensitisers cannot guarantee a therapeutic effect in the clinic, which increases the potential phototoxicity to normal tissues.[23]

To explore the capabilities of the photosensitiser drug delivery system, this study used magnetic mesoporous silica nanoparticles to co-deliver GEM and Ce6, and conducted TEM and fluorescence cellular uptake experiments. It can be seen that Ce6@MSN-Fe_3O_4/GEM@DPM can be efficiently uptaken by pancreatic cancer cells, and the enrichment and effective release of GEM in the cytoplasm and nucleus were achieved. Under light conditions, free Ce6 and Ce6-loaded MSN-Fe_3O_4 nanocomposites significantly induced cell apoptosis and exhibited phototoxicity, with the latter showing a more pronounced effect. Among them, Ce6@MSN-Fe_3O_4/GEM@DPM, with its combined drug toxicity and phototoxicity, demonstrates a more pronounced cell-killing effect.

The aspect ratio of MSNs plays a pivotal role in determining cellular uptake rate and particle quantity.[24] Furthermore, research has revealed that the size and shape of MSNs affect their absorption in cancer cells, with rod-shaped particles being more effective than spherical ones.[25] Consequently, the researcher devised a carrier spiral MSNRs with varying aspect ratios, as a drug delivery system for GEM. The cellular uptake of MSNR was examined to explore their potential as drug carriers. Since spiral MSNRs at different aspect ratios have different surface areas and pore volumes, the authors examined the cytotoxicity of spiral MSNR with a large surface area by studying the cytotoxicity, concentration level, and oxidative stress level of the cells. The experimental results showed that as the concentration of MSNR increased, the cytotoxicity was more pronounced, and the oxidative stress level of cells also increased more obviously.

CONCLUSION

This study has successfully engineered a multifunctional mesoporous silica-based nano-drug co-delivery system that carries both a photosensitiser and GEM within magnetic MSNs. This system offers advantages for drug loading and release, coupled with outstanding superparamagnetic properties, making it suitable for targeted drug delivery and tracking. In *in vitro* experiments, it has demonstrated notable cytotoxicity. However, whether the enhanced antitumour effect is consistent with the *in vitro* results when applied *in vivo* needs to be further investigated.

FUNDING:
This study was supported by the Medical and Health Science and Technology Project of Zhejiang Province (No. 2022KY1202).

ETHICAL APPROVAL:
This study was approved by the Ethics Committee of the Hospital.

PATIENTS' CONSENT:
Not applicable.

COMPETING INTEREST:
The authors declared no conflict of interest.

AUTHORS' CONTRIBUTION:
QL: Wrote the paper, prepared figures, participated in experiments, and contributed to data collection.
SG, MP: Participated in experiments, and contributed to data collection and statistical analysis.
HY: Designed the experiment and made critical revisions to this manuscript.
All authors approved the final version of the manuscript to be published.

REFERENCES

1. Balachandran VP, Beatty GL, Dougan SK. Broadening the impact of immunotherapy to pancreatic cancer: Challenges and opportunities. *Gastroenterology* 2019; **156(7)**:2056-72. doi: 10.1053/j.gastro.2018.12.038.
2. Siegel RL, Miller KD, Wagle NS, Jemal A. Cancer statistics, 2023. *CA Cancer J Clin* 2023; **73(1)**:17-48. doi: 10.3322/caac.21763.
3. Mizrahi JD, Surana R, Valle JW, Shroff RT. Pancreatic cancer. *Lancet* 2020; **395(10242)**:2008-20. doi: 10.1016/s0140-6736(20)30974-0.
4. Chao Y, Liang C, Tao H, Du Y, Wu D, Dong Z, *et al.* Localized cocktail chemoimmunotherapy after *in situ* gelation to trigger robust systemic antitumor immune responses. *Sci Adv* 2020; **6(10)**:eaaz4204. doi: 10.1126/sciadv.aaz4204.
5. Zeng S, Pottler M, Lan B, Grutzmann R, Pilarsky C, Yang H. Chemoresistance in pancreatic cancer. *Int J Mol Sci* 2019; **20(18)**:4504. doi: 10.3390/ijms20184504.
6. Erkan M, Hausmann S, Michalski CW, Fingerle AA, Dobritz M, Kleeff J, *et al.* The role of stroma in pancreatic cancer: Diagnostic and therapeutic implications. *Nat Rev Gastroenterol Hepatol* 2012; **9(8)**:454-67. doi: 10.1038/nrgastro.2012.115.
7. Binenbaum Y, Na'ara S, Gil Z. Gemcitabine resistance in pancreatic ductal adenocarcinoma. *Drug Resist Updat* 2015; **23**:55-68. doi: 10.1016/j.drup.2015.10.002.
8. Dauer P, Nomura A, Saluja A, Banerjee S. Microenvironment in determining chemo-resistance in pancreatic cancer: Neighborhood matters. *Pancreatology* 2017; **17(1)**:7-12. doi: 10.1016/j.pan.2016.12.010.
9. Guan S-W, Lin Q, Yu H-B. Intratumour microbiome of pancreatic cancer. *World J Gastrointest Oncol* 2023; **15(5)**:713-30. doi: 10.4251/wjgo.v15.i5.713.
10. Han H, Li S, Zhong Y, Huang Y, Wang K, Jin Q, *et al.* Emerging pro-drug and nano-drug strategies for gemcitabine-based cancer therapy. *Asian J Pharm Sci* 2022; **17(1)**:35-52. doi: 10.1016/j.ajps.2021.06.001.
11. Cheng Z, Li M, Dey R, Chen Y. Nanomaterials for cancer therapy: Current progress and perspectives. *J Hematol Oncol* 2021; **14(1)**:85. doi: 10.1186/s13045-021-01096-0.
12. Li C, Ma C, Wang F, Xil Z, Wang Z, Deng Y, *et al.* Preparation and biomedical applications of core-shell silica/magnetic nanoparticle composites. *J Nanosci Nanotechnol* 2012; **12(4)**:2964-72. doi: 10.1166/jnn.2012.6428.
13. Slapak EJ, El Mandili M, Bijlsma MF, Spek CA. Mesoporous silica nanoparticle-based drug delivery systems for the treatment of pancreatic cancer: A systematic literature overview. *Pharmaceutics* 2022; **14(2)**:390. doi: 10.3390/pharmaceutics14020390.
14. Tang F, Li L, Chen D. Mesoporous silica nanoparticles: Synthesis, biocompatibility and drug delivery. *Adv Mater* 2012; **24912**:1504-34. doi: 10.1002/adma.201104763.
15. Kankala RK, Han YH, Na J, Lee CH, Sun Z, Wang SB, *et al.* Nanoarchitectured structure and surface biofunctionality of mesoporous silica nanoparticles. *Adv Mater* 2020; **32(23)**: e1907035. doi: 10.1002/adma.201907035.
16. Wan Y, Zhao D. On the controllable soft-templating approach to mesoporous silicates. *Chem Rev* 2007; **107(7)**: 2821-60. doi: 10.1021/cr068020s.
17. Adam A, Mertz D. Iron oxide@mesoporous silica core-shell nanoparticles as multimodal platforms for magnetic resonance imaging, magnetic hyperthermia, near-infrared light photothermia, and drug delivery. *Nanomaterials (Basel)* 2023; **13(8)**:1342. doi: 10.3390/nano13081342.

18. Rascol E, Daurat M, Da Silva A, Maynadier M, Dorandeu C, Charnay C, *et al.* Biological fate of fe(3)O(4) core-shell mesoporous silica nanoparticles depending on particle surface chemistry. *Nanomaterials (Basel)* 2017; **7(7)**:162. doi: 10.3390/nano7070162.

19. Agostinis P, Berg K, Cengel KA, Foster TH, Girotti AW, Gollnick SO, *et al.* Photodynamic therapy of cancer: An update. *CA Cancer J Clin* 2011; **61(4)**:250-81. doi: 10.3322/caac.20114.

20. Lu H, Xu J, Yang J, Wang Z, Xu P, Hao Q, *et al.* On-demand targeting nanotheranostics with stimuli-responsive releasing property to improve delivery efficiency to cancer. *Biomaterials* 2022; **290**:121852. doi: 10.1016/j.biomaterials.2022.121852.

21. Zhang W, Shen J, Su H, Mu G, Sun J-H, Tan C-P, *et al.* Co-delivery of cisplatin prodrug and chlorin e6 by mesoporous silica nanoparticles for chemo-photodynamic combination therapy to combat drug resistance. *ACS Appl Mater Interfaces* 2016; **8(21)**:13332-40. doi: 10.1021/acsami.6b03881.

22. Er O, Tuncel A, Ocakoglu K, Ince M, Kolatan EH, Yilmaz O, *et al.* Radiolabeling, *in vitro* cell uptake, and *in vivo* photodynamic therapy potential of targeted mesoporous silica nanoparticles containing zinc phthalocyanine. *Mol Pharm* 2020; **17(7)**:2648-59. doi: 10.1021/acs.molpharmaceut.0c00331.

23. Navarro JRG, Lerouge F, Cepraga C, Micouin G, Favier A, Chateau D, *et al.* Nanocarriers with ultrahigh chromophore loading for fluorescence bio-imaging and photodynamic therapy. *Biomaterials* 2013; **34(33)**:8344-51. doi: 10.1016/j.biomaterials.2013.07.032.

24. Li L, Huang X, Liu T, Liu H, Hao N, Chen D, *et al.* Overcoming multidrug resistance with mesoporous silica nanorods as nanocarrier of doxorubicin. *J Nanosci Nanotechnol* 2012; **12(6)**:4458-66. doi: 10.1166/jnn.2012.6198.

25. Meng H, Yang S, Li Z, Xia T, Chen J, Ji Z, *et al.* Aspect ratio determines the quantity of mesoporous silica nanoparticle uptake by a small GTPase-dependent macropinocytosis mechanism. *ACS Nano* 2011; **5(6)**:4434-47. doi: 10.1021/nn103344k.